Propellants, Explosives, Pyrotechnics

DOI: 10.1002/prep.201900117

Rheological Behavior of DNAN/HMX Melt-Cast Explosives

Daoli Zhu,[a, b] Lin Zhou,[a] and Xiangrong Zhang*[a]

Abstract: Understanding the rheological behavior of melt-cast explosives is critical for manufacturing melt-cast explosive charges. The research presented herein systematically investigates the rheological behavior of 2,4-dinitroanisole/tetramethylenetetranitra-mine (DNAN/HMX) melt-cast explosive suspensions. The rheological characteristics were measured using a Haake Mars III rheometer. In general, the DNAN/HMX melt-cast explosive suspensions underwent shear-thinning (pseudoplastic) and were strongly affected by solid content, particle size (unimodal distribution), particle gradation (bimodal or multimodal distribution), particle morphology, temperature, and chemical additives. The subsequent measurements and analysis provide important contextual information for designing formulations of DNAN/HMX melt-cast explosives.

Keywords: DNAN/HMX melt-cast explosives · rheological behavior · solid content · particle characteristics · temperature and chemical additives

1 Introduction

The rheological behavior of melt-cast explosives is of particular importance for understanding their pourability. In the manufacturing of melt-cast explosives, the suspensions must flow into a mold to completely fill the cavity; should the suspensions not fill the entire cavity (due to inappropriate rheological behavior), voids or other defects may develop, resulting in shortages in the final products. The rheological behavior of such suspensions in a casting system is governed by the characteristics of both the liquid and solid phases. Generally, the liquid phase presents a Newtonian viscous behavior. However, when the solid phase is dispersed in the liquid phase, the resultant melt-cast explosive suspensions usually present a non-Newtonian viscous behavior and are affected by many factors, such as solid content, particle morphology and size, particle gradation, temperature, and chemical additives.

The rheological behavior of melt-cast explosives has been explored to some extent in previous work, especially for trinitrotoluene-based (TNT-based) melt-cast explosives. The general qualitative law for the rheological behavior of TNT-based melt-cast explosives can be summarized as follows: (1) Molten TNT is similar to a Newtonian fluid [1–3], whereas TNT-based melt-cast explosive suspensions are generally shear-thinning (non-Newtonian) fluids [4–6]. (2) The viscosity of the suspensions increases with increasing solid content [4,7–8]. (3) Given a particular amount of solid content, a reduction in particle size generally results in increased viscosity of the suspensions [4,7,9], whereas suspensions containing particles with a smoother morphology have reduced viscosity [9]. Particle gradation (bimodal or multimodal distribution) is typically used to minimize the viscosity in highly concentrated (high solid content) suspensions [9–10]. (4) The viscosity of the suspensions decreases as the temperature increases [4,7]. Additionally, chemical additives can also change (increase or decrease) the viscosity of the suspensions [8].

Recent developments and characterizations of the performance of insensitive explosives based on DNAN formulations have led to the possible replacement of TNT-based melt-cast explosives in the munitions field. DNAN-based melt-cast explosives have demonstrated the characteristics of equivalent or improved extremely insensitive detonative substances compared with TNT-based melt-cast explosives, while maintaining the performance requirements of explosives [11–12]. The rheological behavior of DNAN-based melt-cast explosives is essential for both its insensitivity and performance. Recently, the rheological behavior of several DNAN-based melt-cast explosives has been investigated and compared with that of TNT-based melt-cast explosives [13–14]. However, a systematic study of the rheological behavior of DNAN-based melt-cast explosives has yet to be reported. Although Meng [15] investigated how numerous factors affect the rheological behavior of DNAN/HMX melt-cast explosives, his investigation considered only low solid content and a limited range of shear rate.

We thus present herein a systematic study of the rheological behavior of DNAN/HMX melt-cast explosive suspensions. The viscosity of the suspensions was measured using

[a] *D. Zhu, L. Zhou, X. Zhang*
State Key Laboratory of Explosion Science and Technology
Beijing Institute of Technology
Beijing 100081, P. R. China
**e-mail: zhangxr@bit.edu.cn*
[b] *D. Zhu*
Anhui Shenjian Polytron Technologies Inc.
Hefei 230000, P. R. China

a Haake rheometer. The effects of solid content, particle size, particle gradation, particle morphology, temperature, and chemical additives on the viscosities of DNAN/HMX suspensions were investigated. The present investigation also provides important contextual information for improving the formulation of DNAN/HMX melt-cast explosives.

2 Experimental Section

2.1 Materials

The DNAN used in this study was supplied by the Dongfang Chemical Industry Group Co., Ltd. (Hubei, China) and used without further purification. The DNAN has a melting point of 94–96 °C and a density of 1.52 g/cm^3, with a purity of 99.6 % $\pm$ 0.3 %.

HMX solid particles of five representative sizes were collected from various sizes of mesh and labeled $S_1 - S_5$ (Yinguang Chemical Industry Group Co.,Ltd, Gansu, China). The particle-size distributions of the samples were determined using a Mastersizer 2000 fitted with a dispersing unit Hydro 2000 MU (Malvern Instruments Ltd., Malvern, UK), which operates based on the laser diffraction principle known as low-angle laser light scattering. The samples were ultrasonicated for approximately 1 minute to prevent the formation of HMX particle agglomerates. Figure 1 shows the particle size distributions of the samples. The mean particle size (d_{50}) of samples $S_1 - S_5$ was 9.1, 23.8, 50.6, 100.7, and 785.3 μm, respectively. The samples were generally nonspherical; however, they could be further spheroidized. A typical spheroidized sample $S_3^{'}$ was prepared by recrystallization and then sifted out, ensuring that $S_3^{'}$ and S_3 had nearly the same particle-size distribution (d_{50} of $S_3^{'}$ is 50.2 μm, the particle-size distribution of $S_3^{'}$ is not completely overlapped with that of S_3, however, these negligible differences between S_3 and $S_3^{'}$ are not shown in Figure 1). Scanning electron microscopy (SEM, Tescan MIRA3 XMU, Czech Republic) was used to analyze the morphology of samples S_3 (nonspherical) and $S_3^{'}$ (spheroidized). As shown in Figure 2, the spheroidized particles ($S_3^{'}$) had a much more regular shape than the nonspherical particles (S_3).

The three typical chemical additives (MNA, CAB, and TPU 5702) used in this work are given in Table 1.

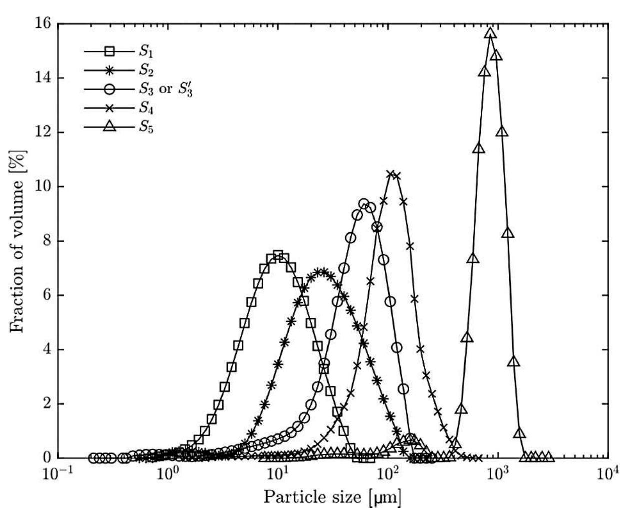

Figure 1. Particle-size distribution of the five samples.

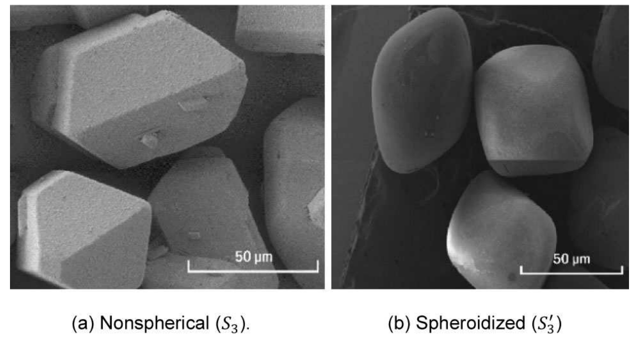

(a) Nonspherical (S_3). (b) Spheroidized (S_3')

Figure 2. Morphological characterization of S_3 and $S_3^{'}$.

Table 1. Chemical additives.

Chemical name	Abbreviation	Density/ g·cm^{-3}	Source
N-methyl-4-nitro-aniline	MNA	1.26	Dongfang Chemical Industry Group Co., Ltd
Cellulose acetate butyrate	CAB	1.39	Kai Yin, Shanghai Chemical Co., Ltd
Thermoplastic polyurethanes 5702	TPU 5702	1.19	Lubrizol Shanghai FTZ Trading Operation

2.2 Sample Preparation and Viscosity Measurement

DNAN was first melted at 100 °C in a double-jacketed stainless-steel kettle equipped with a stirrer. The HMX solid was then added incrementally to the molten DNAN and stirred at a rate of 200–300 rev/min. After adding the solid to the DNAN, the mixture was stirred for 15 minutes at a rate of 500 rev/min to ensure uniform mixing and to eliminate any solid agglomerates.

The rheological behavior of the DNAN/HMX suspensions was determined using an R/S Haake Mars III rheometer (Thermo Fisher Scientific Inc., Waltham, MA, USA) equipped with a temperature-control unit. The temperature of the measuring cylinder was controlled at an accuracy of $\pm$0.02 °C by using a Thermo Fisher circulating oil bath. The measuring element has a Couette geometry with a gap of

1.7 or 6.0 mm. The gap of 1.7 mm is used for rheological measurements of samples $S_1 - S_4$, while the gap of 6.0 mm is used for rheological measurements related to sample S_5. These gaps are sufficiently large to minimize possible artificial wall effects [16]. However, for the gap of 6.0 mm, the assumption of constant shear rate in the gap may not be completely respected.

2.3 Sedimentation and Precaution

Before investigating how solid content, particle size, particle gradation, particle morphology, temperature, and chemical additives affect the rheological behavior of DNAN/HMX suspensions, we first observed and analyzed the particle-sedimentation phenomenon. As shown in Figure 3, the sedimentation effect is negligibly small for the typical fine particles (S_1 and S_3) but is much more significant for the typical coarse particles (S_5). Assuming that the sedimentation process can be described by Stokes flow [17], then the sedimentation velocity v for a single particle is $(\rho_s - \rho_0)gd^2/18\eta_0$, where ρ_s is the particle density, ρ_0 is the solvent density, η_0 is the solvent viscosity, g is the acceleration due to gravity, and d is the particle diameter. Therefore, the sedimentation effect increases sharply with increasing particle size ($v \propto d^2$).

To reduce the influence of particle sedimentation, all measurements were performed on fine particles (S_3) except for measurements designed to investigate how particle size and particle gradation affect the rheological behavior of DNAN/HMX suspensions. Moreover, because sedimentation velocity is inversely proportional to solvent viscosity ($v \propto 1/\eta_0$) and η_0 decreases with increasing temperature, experiments are better done at lower temperatures. In the present study, all measurements were made at 100 °C with the exception of measurements required to analyze how temperature affects the rheological behavior of DNAN/HMX suspensions. Additionally, all measurements lasted a maximum of 10 minutes to ensure that sedimentation effects were negligible (Figure 3).

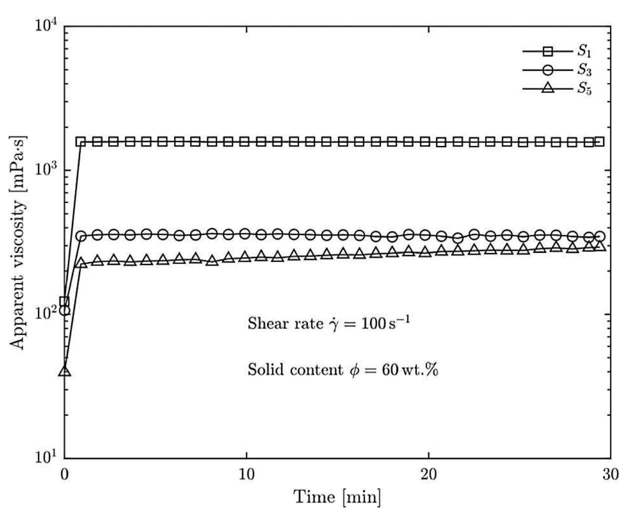

Figure 3. Effect of sedimentation on viscosity measurements.

3 Results and Discussion

3.1 Effect of Solid Content on the Rheological Behavior of DNAN/HMX Suspensions

Figure 4 shows the viscosity of DNAN/HMX suspensions with various solid contents. When the solid content $\phi \leq 3$ wt.%, the DNAN/HMX suspensions present nearly Newtonian viscous behavior. However, when the solid content $\phi \geq 10$ wt.%, the apparent viscosity of the DNAN/HMX suspensions decreases exponentially with shear rate, in-

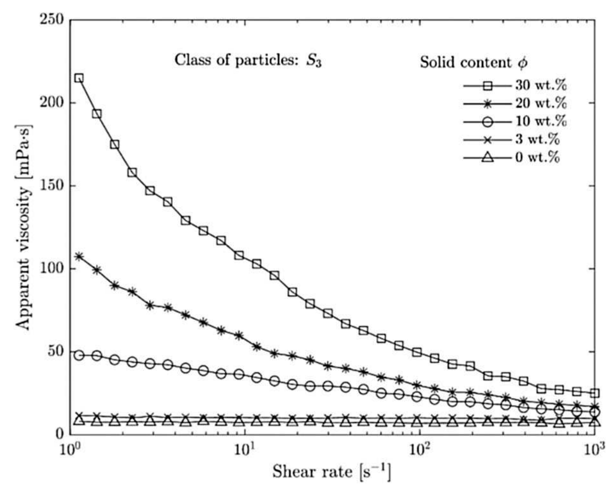

(a) $0 \leq \phi \leq 30$wt.%

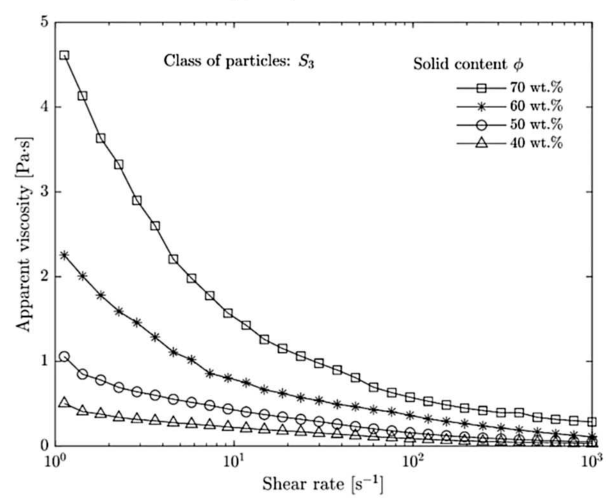

(b) $40 \leq \phi \leq 70$wt.%

Figure 4. Apparent viscosities of DNAN/HMX suspensions with different solid contents

dicating non-Newtonian (shear thinning) viscous behavior. Moreover, at a given shear rate, the apparent viscosity of the DNAN/HMX suspensions increases with increasing solid content. Generally, particles in a liquid act as obstacles, hindering the liquid flow and therefore increasing the flow resistance (i.e., the viscosity). With increasing solid content, the separation between particles decreases [18], so it is more likely that particles collide, and more additional shear force is required when friction occurs during particle collision. In addition, at low shear rate, the difference between the apparent viscosity of high and low solid content becomes prominent. However, this difference is less prominent at higher shear rate because particles become favorably aligned with the flow direction [16,19].

The relationship between the apparent viscosity of the suspension and the shear rate can be approximated by using the following power-law model [20]:

$$\eta = K\dot{\gamma}^{n-1} \tag{1}$$

where η is the apparent viscosity, $\dot{\gamma}$ is the shear rate, and K and n are empirical curve-fitting parameters known as the fluid consistency coefficient and the flow-behavior index, respectively [20]. When $n < 1$, the suspension exhibits shear-thinning behavior; when $n > 1$, the suspension exhibits shear-thickening behavior; and when $n = 1$, the suspension exhibits Newtonian behavior. The value of K can be interpreted as the value of apparent viscosity at unity shear rate. As shown in Table 2, the consistency coefficient K of DNAN/HMX suspensions increases with increasing solid content; however, the flow-behavior index n decreases with increasing solid content, indicating an increasing degree of shear thinning. Additionally, when the solid content $\phi \leq 3$ wt.%, the index n is close to 1, again indicating the nearly Newtonian behavior of these suspensions. However, the coefficient of determination R^2 for $\phi \leq 3$ wt.% is much smaller than for $\phi \geq 10$ wt.%, which demonstrates that the power-law model (Eq. (1)) is not optimal when $\phi \leq 3$ wt.%. Instead, a linear model may be a better choice to relate η and $\dot{\gamma}$ or η and ϕ. However, this discussion is not broached herein.

Table 2. Parameters for power-law model of DNAN/HMX suspensions with various solid contents.

ϕ/wt.%	K/mPa · s^n	n	R^2
0	7.8	0.9828	0.4679
3	10.8	0.9797	0.6369
10	51.5	0.8207	0.9894
20	108.6	0.7203	0.9980
30	214.6	0.6819	09969
40	485.9	0.6369	0.9897
50	1024.2	0.6011	0.9910
60	2299.2	0.5608	0.9955
70	4813.7	0.5229	0.9973

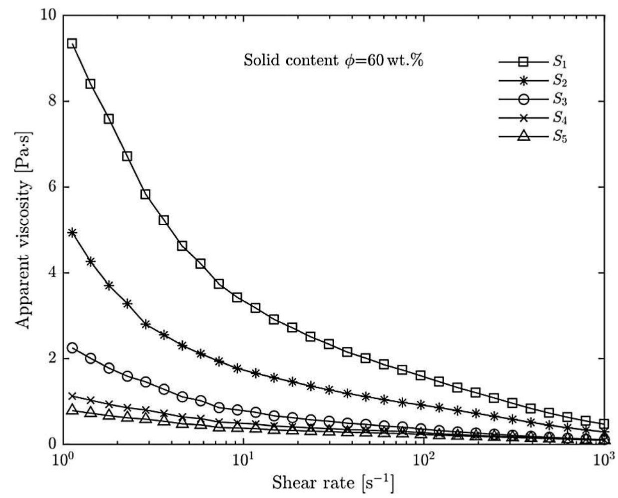

Figure 5. Effect of particle size on the apparent viscosity of DNAN/HMX suspensions.

3.2 Effect of Particle Size, Particle Gradation, and Particle Morphology on Rheological Behavior of DNAN/HMX Suspensions

Figure 5 shows how particle size (unimodal distribution) affects the apparent viscosity of DNAN/HMX suspensions. The apparent viscosities of DNAN/HMX suspensions clearly decrease as d_{50} increases for HMX. When the solid content is high, particle-particle interactions become significant. Moreover, at a given solid content, the total particle number in a suspension increases with decreasing particle size, resulting in a higher influence of inter-particle friction, thereby inducing higher viscosity [21]. However, when d_{50} for HMX particles exceeds 100 μm, as is the case for S_4 and S_5 in Figure 5, particle size has only a negligible effect on apparent viscosity. This phenomenon is similar to what occurs in TNT-based melt-cast explosives [9]. In addition, the difference in viscosity between fine and coarse particles decreases at higher shear rates, which may also be attributed to particles being favorably rearranged with respect to the flow direction [16].

One important implication from Figure 5 is that coarse particles are preferable to obtain a suspension with a high solid content. However, as pointed out in Section 2.3, coarse particles are subject to a much more serious sedimentation effect than fine particles. In addition, coarse particles alone are not advantageous to achieve a higher solid content. A better approach is to mix coarse and fine particles together (particle gradation) because it gives a broader particle-size distribution (bimodal or multimodal) so that fine particles may fit into the spaces between packed coarse particles [22]. Particle gradation can strongly affect suspension viscosity; a generally optimized gradation is capable of minimizing viscosity [23–24]. Furthermore, particle gradation is believed to be affected by two crucial process

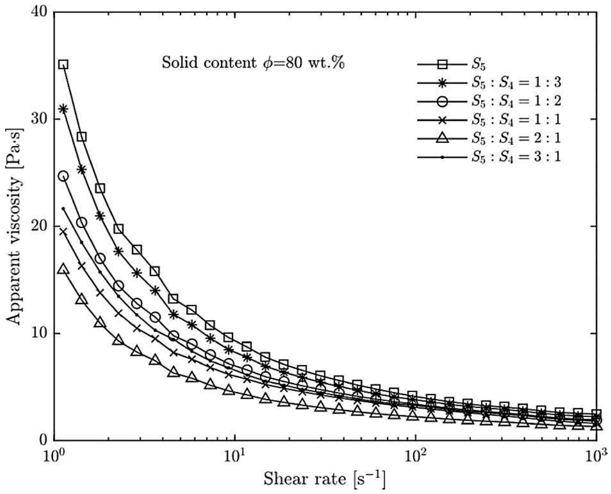

Figure 6. Effect of particle gradation on apparent viscosity of DNAN/HMX suspensions.

parameters [23]: (i) the ratio λ of the diameter (d_{50} in the present study) of coarse particles to that of fine particles, and (ii) the ratio ζ of the mass of coarse particles to that of fine particles.

Figure 6 shows how particle gradation affects the apparent viscosity of DNAN/HMX suspensions. The best parameter for ζ is about 2 when samples S_5 ($d_{50} = 785.3$ µm) and S_4 ($d_{50} = 100.7$ µm) (λ is about 8) are mixed to obtain high solid content ($\phi = 80$ wt.%). In contrast, for HTPB/CL-20 casting explosives, the optimal value of ζ is 3 when CL-20 particles with diameters 30 and 2 µm (λ is 15) are mixed to minimize viscosity [25].

Figure 7 shows how particle morphology affects the apparent viscosity of DNAN/HMX suspensions. Although spheroidized particles $S_3^{'}$ and nonspherical particles S_3 (Figure 2) have nearly the same size distribution (Figure 1), the apparent viscosity of the suspension with spheroidized particles is less than that with nonspherical particles. In general, given a certain particle-size distribution, small particles can fit into the gaps between large particles. However, nonspherical particles will lead to poorer space-filling than spheroidized particles and thus higher viscosity [26].

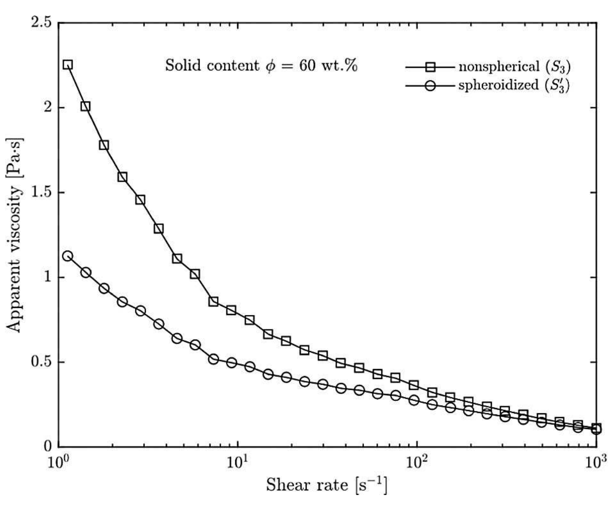

Figure 7. Effect of particle morphology on apparent viscosity of DNAN/HMX suspensions.

3.3 Effect of Temperature and Chemical Additives on Rheology of DNAN/HMX Suspensions

The viscosity for a liquid decreases with increasing temperature. For a solid-liquid suspension, the effect of temperature on the apparent viscosity is similar. As shown in Figure 8, the apparent viscosity of the DNAN/HMX suspensions decreases with increasing temperature. The effect of temperature is fit to the Arrhenius relationship [6]

$$\eta = Ae^{\frac{E}{RT}} \tag{2}$$

where E is the activation energy for flow, T is the absolute temperature, A is a constant, and R is the universal gas constant. As shown in Table 3, the activation energy E for suspensions with high solid content is greater than for suspensions with lower solid contents. Furthermore, based on Eq. (2), the derivative $\mathrm{d}\eta/\mathrm{d}T$ of viscosity with respect to

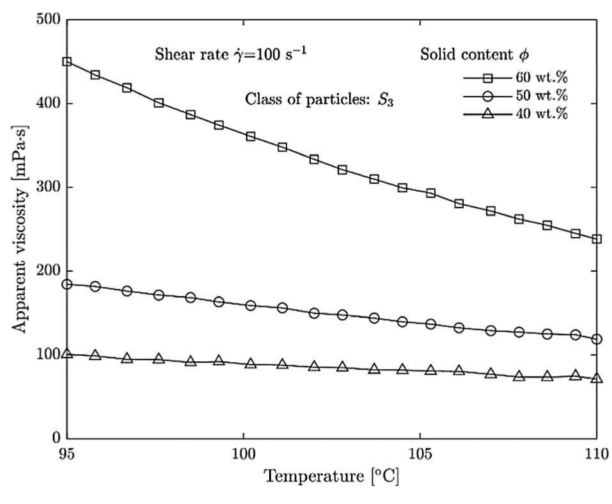

Figure 8. Apparent viscosity of DNAN/HMX suspensions as a function of temperature and for different solid contents.

Table 3. Arrhenius parameters for DNAN/HMX suspensions with different solid contents.

ϕ/wt.%	A/mPa·s	E/kJ·mol^{-1}	R^2
40	2.36E-2	25.55	0.9860
50	2.50E-3	34.33	0.9977
60	4.53E-5	49.30	0.9997

temperature can be easily obtained, and the absolute value of $d\eta/dT$ increases as E increases, indicating that viscosity is more sensitive to changes in temperature at high solid content than at low solid content.

Chemical additives are typically necessary to provide certain required properties of melt-cast explosives. MNA is typically used to lower the melting point of DNAN [27], and CAB and TPU 5702 are often used to improve the mechanical properties of melt-cast explosives. In addition, these chemical additives exert an additional effect on the rheological behavior of the melt-cast explosive suspension. As shown in Figure 9, although a small quantity of chemicals are added, it strongly affects the apparent viscosity of DNAN/HMX suspensions. Furthermore, the apparent viscosity of DNAN/HMX suspensions decreases with increasing quantity of MNA, whereas it increases with increasing quantity of CAB and TPU 5702.

4 Conclusions

The rheological behavior of DNAN/HMX melt-cast explosives was measured using a Haake rheometer at shear rates up to 1000 s^{-1}. We thoroughly investigated how six factors (solid content, particle size, particle gradation, particle morphology, temperature, and chemical additives) affect the apparent viscosities of DNAN/HMX melt-cast explosive suspensions. The results show that (1) the apparent viscosity increases with increasing solid content. When the solid content $\phi \leq 3$ wt.%, the viscosity of the DNAN/HMX suspensions is nearly Newtonian. However, when the solid content $\phi \geq 10$ wt.%, the apparent viscosity of the DNAN/HMX suspensions decreases exponentially with shear rate, which can be described by a power-law model. (2) At a given solid content, the apparent viscosity of DNAN/HMX suspensions decreases as the mean particle size (unimodal distribution) of HMX increases. However, when d_{50} for the HMX particles exceeds 100 μm, particle size has little effect on the apparent viscosity of DNAN/HMX suspensions. (3) Particle gradation (bimodal or multimodal distribution) is required to increase the solid content. In the present study, the ratio of the mass of the coarse particles ($d_{50} = 785.3$ µm) to that of the fine particles ($d_{50} = 100.7$ µm) is 2:1, which minimizes the viscosity of the DNAN/HMX suspensions, and the solid content can reach up to 80 wt.%. (4) Particle morphology strongly affects the viscosity of DNAN/HMX suspensions, and the apparent viscosity of the suspension with spheroidized particles is less than that with nonspherical particles. (5) The effect of temperature on the viscosity of the DNAN/HMX suspensions can be described by an Arrhenius equation. The apparent viscosity decreases as the temperature increases, and becomes increasingly sensitive to temperature with higher solid content. (6) Chemical additives strongly affect the viscosity of DNAN/HMX suspensions. The apparent viscosity decreases with increasing quantity of MNA,

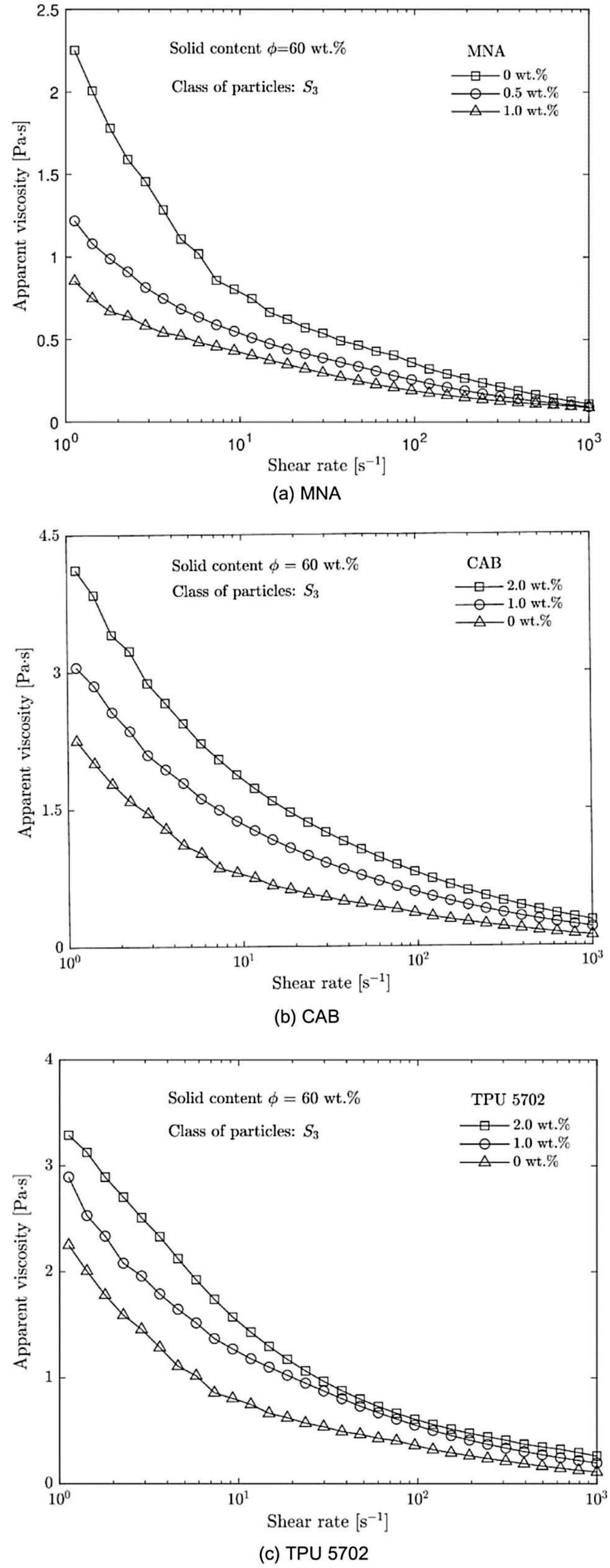

Figure 9. Effect of additives on the apparent viscosity of DNAN/HMX suspensions.

whereas it increases with increasing quantity of CAB and TPU 5702. Overall, the qualitative rheological behavior of DNAN-based melt-cast explosives is similar to that for TNT-based melt-cast explosives. However, for designing specific formulations of DNAN/HMX melt-cast explosives, this investigation provides important benchmarks for further optimization.

Acknowledgement

This study was supported by the National Natural Science Foundation of China (Grant No. 11772060).

References

[1] M. A. Parry, H. H. Billon, A note on the coefficient of viscosity of pure molten 2,4,6-trinitrotoluene (TNT), *Rheol. Acta* **1988**, *27*, 661–663.

[2] M. A. Parry, H. H. Billon, Flow behaviour of molten 2,4,6-trinitrotoluene (TNT) between concentric cylinders, *Rheol. Acta* **1990**, *29*, 462–468.

[3] J. P. Guillemin, L. Brunet, O. Bonnefoy, G. Thomas, A flow time model for melt-cast insensitive explosive process, *Propellants Explos. Pyrotech.* **2007**, *32*, 261–266.

[4] V. S. Joshi, S. Vadali, R. D. Wasnik, S. K. Jangid, M. Maurya, Studies on rheological properties and process parameters of TNT based castable high explosive compositions, *Sci. Technol. Energ. Mater.* **2017**, *78*, 87–92.

[5] D. K. Zerkle, M. P. Núñez, J. M. Zucker, Molten composition B viscosity at elevated temperature, *J. Energ. Mater.* **2016**, *34*, 368–383.

[6] R. Sarangapani, V. Ramavat, S. Reddy, P. Subramanian, A. K. Sikder, Rheology studies of NTO-TNT based melt-cast dispersions and influence of particle-dispersant interactions, *Powder Technol.* **2015**, *273*, 118–124.

[7] H. Q. Li, C. W. An, W. J. Guo, Y. J. Wei, H. X. Li, J. Y. Wang, Study on rheological properties of DNTF/TNT/HMX based on melt-cast explosive, *J. North Univ. China (Nat. Sci. Ed.)* **2014**, *35*, 720–723 and 728.

[8] G. G. Xu, J. P. Xu, Rheological properties of TNT/RDX suspensions, *Acta Armamentarii.* **1991**, *12*, 71–74.

[9] B. Singh, D. R. Kaushik, Spheroidization of RDX and its effect on the pourability of RDX/TNT slurries, *Def. Sci. J.* **1989**, *39*, 95–98.

[10] H. H. Billon, M. A. Parry, The viscosity of TATB types A and B suspensions in molten TNT: General characteristics, *Tech. rep.*, Materials Research Labs Ascot Vale, Commonwealth Australia, **1991**.

[11] S. Nicolich, J. Niles, D. Doll, M. Ray, M. Gunger, A. Spencer, Development of a novel high fragmentation/high blast melt pour explosive, in: *Proceedings of the 2003 Insensitive Munitions & Energetic Materials Symposium*, Orlando, FL, USA, March 10–13, **2003**.

[12] P. J. Davies, A. Provatas, *Characterisation of 2,4-dinitroanisole: An ingredient for use in low sensitivity melt cast formulations, DSTO-TR-1904, Defense Science and Technology Organization*, Edinburgh South Australia, **2006**.

[13] P. Pelletier, I. Laroche, D. Lavigne, F. Cantin, P. Brousseau, V. Fung, Processing studies of DNAN-based melt-pour explosives formulations, *Insensitive Munitions and Energetic Materials Technology Symposium,* Tucson, AZ, USA, **2009**, May 11–14.

[14] A. Provatas, P. J. Davies, Australian melt-cast explosives R&D, DNAN–A replacement for TNT in melt-cast formulations, *Insensitive Munitions and Energetic Materials Technology Symposium,* Bristol, UK, April 24–28, **2006**.

[15] J. J. Meng, L. Zhou, D. Y. Jin, S. T. Cao, Q. H. Wang, Rheological properties of DNAN/HMX melt cast explosives, *Chin. J. Energet. Mater.* **2018**, *26*, 677–685.

[16] F. Chinesta, G. Ausias, *Rheology of Non-spherical Particle Suspensions*, Elsevier, Oxford, **2015**.

[17] F. A. Morrison, *An introduction to fluid mechanics*, Cambridge University Press, New York, **2013**.

[18] S. Mueller, E. W. Llewellin, H. M. Mader, The rheology of suspensions of solid particles, *P. Ro. Soc Lond. A Math.* **2010**, *466*, 1201–1228.

[19] J. Mewis, N. J. Wagner, *Colloidal suspension rheology*, Cambridge University Press, New York, **2012**.

[20] R. P. Chhabra, J. F. Richardson, *Non-Newtonian flow and applied rheology: engineering applications*, Butterworth-Heinemann, Oxford, **2008**.

[21] N. S. Roh, D. H. Shin, D. C. Kim, J. D. Kim, Rheological behaviour of coal-water mixtures. 1. effects of coal type, loading and particle size, *Fuel* **1995**, *74*, 1220–1225.

[22] J. J. Stickel, R. L. Powell, Fluid mechanics and rheology of dense suspensions, *Annu. Rev. Fluid Mech.* **2005**, *37*, 129–149.

[23] J. S. Chong, E. B. Christiansen, A. D. Baer, Rheology of concentrated suspensions, *J. Appl. Polym. Sci.* **1971**, *15*, 2007–2021.

[24] A. J. Poslinski, M. E. Ryan, R. K. Gupta, S. G. Seshadri, F. J. Frechette, Rheological behavior of filled polymeric systems ii. the effect of a bimodal size distribution of particulates, *J. Rheol.* **1988**, *32*, 751–771.

[25] H. X. Li, J. Y. Wang, C. W. An, Study on the rheological properties of CL-20/HTPB casting explosives, *Cent. Eur. J. Energ. Mater.* **2014**, *11*, 237–255.

[26] H. A. Barnes, J. F. Hutton, K. Walters, *An introduction to rheology*, Elsevier, New York, **1989**.

[27] D. L. Zhu, L. Zhou, X. R. Zhang, J. Y. Zhao, Simultaneous determination of multiple mechanical parameters for a DNAN/HMX melt-cast explosive by brazilian disc test combined with digital image correlation method, *Propellants Explos. Pyrotech.* **2017**, *42*, 864–872.

Manuscript received: April 8, 2019
Revised manuscript received: August 3, 2019
Version of record online: September 5, 2019

